JOURNAL OF GEOPHYSICAL RESEARCH, VOL. 89, NO. B12, PAGES 10,365–10,373, NOVEMBER 10, 1984

Coupled Thermal-Hydraulic-Mechanical Phenomena in Saturated Fractured Porous Rocks: Numerical Approach

J. NOORISHAD, C. F. TSANG, AND P. A. WITHERSPOON

Earth Sciences Division, Lawrence Berkeley Laboratory, University of California, Berkeley

The fundamentals of the theory of consolidation and thermoelasticity are recast into the formulation of a phenomenon called thermohydroelasticity. Subsequently, a variational principle and Galerkin formulation are combined with the finite element method to develop a new technique to investigate coupled thermal-hydraulic-mechanical behavior of liquid-saturated, fractured porous rocks. A code-to-code verification of the method is performed. Finally, the environment of a heater emplaced in hard rock is simulated. The effects of the coupled thermal stresses in the fractured rock are evident from the dramatic reduction of permeability due to the deformation of the fractures. These results can improve the understanding of observations and displacement measurements made in the in situ experiments at the Stripa mine in Sweden.

INTRODUCTION

The presence of heat in a liquid-saturated geologic medium brings about a chain of events that is caused by what are referred to as coupled thermal-hydraulic-mechanical phenomena. The interdependence of each of these three phenomena leads to a coupled behavior that is very complex. However, recent progress in coupled analyses among pairs of these three phenomena provides a basis for treating all three phenomena in a fully coupled manner. In this paper, we first review the developments for coupled hydromechanical, hydrothermal, and thermomechanical processes and then present the fully coupled problem.

Hydraulic behavior of saturated porous media has been studied for a long time, and excellent reviews can be found in recent publications [*Weeks*, 1977; *Freeze and Cherry*, 1979]. In the usual treatment of fluid flow in porous media, deformation of the medium is considered by introducing a coefficient of specific storage [*Theis*, 1938]. This approach, although by no means precise, is adequate to represent most fluid flow problems. However, the well-known theory of consolidation, introduced by *Terzaghi* [1925], which is mainly used for settlement analysis, was the first rigorous means of analyzing the effects of deformability on flow of fluid in a medium. Terzaghi introduced the concept of effective stress and accounted for the coupling of fluid flow and deformation of the solids. *Biot* [1941] introduced a more general theory of consolidation that makes possible a more realistic treatment of the hydromechanical behavior of saturated porous rocks. The early work of *Biot* [1941] appeared to be physically motivated but was later supplemented by a thermodynamic base [*Biot*, 1956].

The theories of mixtures [e.g., *Green and Naghdi*, 1965; *Crochet and Naghdi*, 1966; *Aifantis*, 1977] have a sound thermodynamic base and a general associated constitutive theory. They provide a basis for developing, as a special case, a theory for flow of fluids through porous elastic solids that is equivalent to Biot's result.

For a long time, solution techniques for hydromechanical problems lagged behind theory and were restricted to simple geometries. With the advent of computers, numerical solution techniques were developed for coupled one-dimensional equations of consolidation and multidimensional equations of fluid flow. This provided an approximate means of analyzing general fluid flow problems in deformable porous media [*Helm*, 1974; *Narasimhan and Witherspoon*, 1977]. In an attempt to develop a method for the solution of general consolidation problems, *Sandhu and Wilson* [1969] applied the variational finite element method to the problem of fluid flow through saturated, porous elastic solids. This method was extended by *Ghaboussi and Wilson* [1973], who considered the effects of fluid compressibility.

Recently, *Safai and Pinder* [1979] developed a Galerkin finite element method of analyzing fluid flow through deformable porous media and made an attempt to consider the entire saturated-unsaturated flow regime. The proper constitutive stress-strain relationships for the extension of *Biot*'s [1941] theory to the entire flow regime was later provided by *Noorishad et al.* [1982*b*].

Unlike soils (porous media), which exhibit the dramatic settlement behavior that motivated the development of consolidation theories, fractures and the effects of their deformation went unnoticed until recently. *Davis and Moore* [1965] presented one of the first direct measurements of fracture deformation (of the order of microns) caused by earth tides. *Snow* [1968] reported strains of 10^{-7} to 10^{-8} at a distance of about 300 ft (91.4 m) from a water well in metamorphic rocks subjected to 30 ft (9.14 m) of drawdown. More indirect evidence of fracture deformation has accumulated from (1) the difference between pumping into and pumping out of a well [*Evans*, 1966], (2) the nonlinear relationship between fluid pressure and flow rate during injection tests [*Snow*, 1965; *Louis and Maini*, 1970], and (3) the pressure dependence of transmissivity in the Precambrian reservoir beneath the Denver Basin [*Van Poollen*, 1969]. For some time, hydraulic and hydromechanical analyses of fractures were achieved using an equivalent porous medium approach. *Noorishad* [1971] conducted theoretical and numerical studies of fluid flow in a rock mass, taking into account the deformable nature of fractures in a discrete manner. This work was based on earlier studies of discrete fracture behavior from a load-deformation point of view by *Goodman et al.* [1968] and a fluid flow point of view by *Wilson and Witherspoon* [1970]. Further laboratory and field tests by *Gale* [1975] provided strong evidence of nonlinear fracture deformability induced by fluid pressure changes and also verified the capability of earlier numerical solution techniques [*Noorishad*, 1971].

Paper number 4B0983.
0148-0227/84/004B-0983$05.00

A deterministic solution for transient flow of fluids in deformable fractured porous rocks was not achieved until recently. *Ayatollahi* [1978] has used an enumerative approach that is based upon a generalization of *Biot*'s [1941] constitutive stress-strain law and incorporates a *Gurtin* [1964] type variational principle. An extension of this work by *Noorishad et al.* [1982*a*] provides a general two-dimensional finite element solution technique for the study of the deformation, stress distribution, fluid storage, and hydraulic properties of a fractured porous medium under the influence of fluid flow and structural boundary conditions. Reviews of other recent efforts to develop hydromechanical models are also available [*Baca*, 1980; *Tsang*, 1980].

Coupled phenomena of fluid flow and heat flow, usually known as hydrothermal flow, have been the subject of detailed studies. Recent accounts of the state of the art can be found in the works by *Pinder* [1979] and *Wang et al.* [1980].

Study of thermal effects on linear and nonlinear elastic materials, known as thermoelasticity, is a discipline that has been thoroughly covered in physics and engineering and need not be considered here. As far as rock mechanics usage is concerned, thermoelasticity lies mostly within the confines of continuum applications. An account of the status and needs of the thermomechanical modeling techniques for continuous and discontinuous media is given by *Hocking* [1979]. More recent reports [*Baca*, 1980; *Tsang*, 1980] indicate that some models being developed either have provisions for incorporating fractures in them or actually have the capability for deterministically modeling discontinuous media.

The studies cited above have each focused on only two aspects of a much broader question that needs investigation. This is the fully coupled problem of how to analyze the behavior of a fractured rock mass that is subject to the effects of thermal, hydraulic, and mechanical perturbations. We shall refer to the combined effects as thermohydroelasticity. From reviews by *Atherton et al.* [1976], *Baca* [1980], *Miller et al.* [1980], and *Wang et al.* [1980] it appears that a number of workers [e.g., *Pritchett et al.*, 1975; *Bear and Corapcioglu*, 1981] have been and are considering the fully coupled problem of thermohydroelasticity, but to our knowledge very little on this subject has appeared in the literature. One case of interest has recently been reported by *Aboustit et al.* [1982]. They have developed a variational formulation for the coupled thermal-hydraulic-mechanical behavior of elastic porous media. However, the role of convection in the transfer of energy had to be disregarded, and the contributions of the compressibility and thermal expansion of the fluid were not considered. Only an indirect coupling between the energy and fluid flow equations resulted.

This work is the result of our effort to treat the fully coupled problem of thermohydroelasticity and is a natural outgrowth of earlier work in this laboratory. We first present the fundamental equations and then define the initial and boundary conditions. Because of the complexity of the problem, we have not attempted an analytical solution. Therefore this paper is concerned with a numerical solution and the development of a finite element code, ROCMAS, that is based on a mixed variational and Galerkin approach. A partial verification of the code was reported earlier [*Witherspoon et al.*, 1981*b*], and a code-to-code comparison utilizing the results of *Aboustit et al.* [1982] will be presented here. Also discussed are the results of an application, the simulation of the environment of an emplaced heater. A second paper will be prepared when comprehensive application studies of this work become available.

FIELD EQUATIONS

The displacement field within a saturated, porous elastic medium is defined by two field variable quantities; $\mathbf{U}_l$ and $\mathbf{U}_s$, which represent displacement vectors of the fluid and the solid, respectively. The velocity field vectors are correspondingly defined as $\mathbf{V}_l$ and $\mathbf{V}_s$, leading to the representation of the fluid relative velocity as

$$\mathbf{V}_r = \mathbf{V}_l - \mathbf{V}_s \tag{1}$$

Using (1) in the Eulerian form of the mass balance equation, given in the absence of a source term as [*Mercer*, 1973]

$$\frac{\partial \hat{\rho}_l}{\partial t} + \nabla \cdot \hat{\rho}_l \mathbf{V}_l = 0 \tag{2}$$

yields

$$\frac{\partial \hat{\rho}_l}{\partial t} + \hat{\rho}_l \nabla \cdot \mathbf{V}_s + \mathbf{V}_s \cdot \nabla \hat{\rho}_l + \nabla \cdot \hat{\rho}_l \mathbf{V}_r = 0 \tag{3}$$

where

$$\hat{\rho}_l = \phi \rho_l$$

and ϕ and ρ_l are the porosity of the medium and the fluid mass density, respectively. Employing the comoving time derivative, for following the motion of a solid particle along its trajectory, expressed as

$$\frac{D}{D^s t} = \frac{\partial}{\partial t} + \mathbf{V}_s \cdot \nabla \tag{4}$$

in (3) results in the following form of the continuity equation:

$$\frac{D\hat{\rho}_l}{D^s t} + \hat{\rho}_l \nabla \cdot V_s + \nabla \cdot \hat{\rho}_l V_r = 0 \tag{5}$$

Similarly, the Lagrangian form of the differential mass balance for the solid is obtained as

$$\frac{D\hat{\rho}_s}{D^s t} + \hat{\rho}_s \nabla \cdot \mathbf{V}_s = 0 \tag{6}$$

This equation provides an important relationship for use in (5) as follows. Substitution of $\hat{\rho}_s(1 - \phi)\rho_s$, with ρ_s being constant, in (6) results in

$$\frac{1}{1 - \phi} \frac{D\phi}{D^s t} = \nabla \cdot \mathbf{V}_s \tag{7}$$

However, $\nabla \cdot \mathbf{V}_s$ can be expressed in terms of skeleton volume strain e as

$$\nabla \cdot \mathbf{V}_s = \frac{\partial}{\partial t} \nabla \cdot \mathbf{U}_s = \frac{\partial}{\partial t} (\delta_{ij} e_{ij}) = \frac{\partial e}{\partial t} \tag{8}$$

Accordingly, (7) can be written as

$$\frac{D\phi}{D^s t} = (1 - \phi) \frac{\partial e}{\partial t} \tag{9}$$

Substitution of (8) and (9) in (5), along with simple manipulations, results in a new form for the relative mass balance equation for the fluid,

$$\phi \frac{D\rho_l}{D^s t} + \rho_l \frac{\partial e}{\partial t} + \nabla \cdot \hat{\rho}_l \mathbf{V}_r = 0 \tag{10}$$

Development of the momentum balance for the fluid flow in porous media under usual assumptions [*Mercer*, 1973] yields the generalized Darcy equation of motion in the Cartesian coordinate system:

$$\mathbf{q} = -\frac{\mathbf{k}_f}{\eta_l} \cdot (\nabla P + \rho_l g \nabla z) \tag{11}$$

where

η_l liquid dynamic viscosity;
$\mathbf{q}$ $\phi \mathbf{V}_r$;
$\mathbf{k}_f$ local intrinsic permeability tensor;

$$\nabla z = \begin{Bmatrix} 0 \\ 0 \\ 1 \end{Bmatrix};$$

P liquid pressure.

Substitution of (11) in (10) yields the following equation:

$$\phi \frac{D\rho_l}{D^s t} + \rho_l \frac{\partial e}{\partial t} = \nabla \cdot \frac{\rho_l \mathbf{k}_f}{\eta_l} \cdot (\nabla P + \rho_l g \nabla z) \tag{12}$$

Further development of (12) requires the fluid state equation relating fluid density to temperature and pressure. Assuming small changes of density, the truncated Taylor series expansion of ρ_l about the reference density ρ_0 provides the required relationship:

$$\rho_l = \rho_0 + \left(\frac{\partial \rho_l}{\partial T}\right)_0 (T - T_0) + \left(\frac{\partial \rho_l}{\partial P}\right)_0 (P - P_0) \tag{13}$$

The coefficients in the above equation can be defined as

$$\beta_T = \frac{(\partial \rho_l / \partial T)_0}{\rho_0} \qquad \beta_P = \frac{(\partial \rho_l / \partial P)_0}{\rho_0}$$

where β_T is the coefficient of thermal volume expansion for the liquid and β_P is the compressibility coefficient of the liquid. Substituting β_T and β_P in (13) and taking the comoving time derivative of the fluid density, with respect to solid velocity, gives

$$\frac{D\rho_l}{D^s t} = \rho_0 \beta_T \frac{DT}{D^s t} + \rho_0 \beta_P \frac{DP}{D^s t} \tag{14}$$

Using (14) in (12) and neglecting the $\mathbf{V}_s \cdot \nabla P$ and $\mathbf{V}_s \cdot \nabla T$ terms yields

$$\frac{\partial \xi}{\partial t} - \frac{e}{\rho_0} \frac{\partial \rho_l}{\partial t} = \nabla \cdot \left[\frac{\rho_l \mathbf{k}_f}{\rho_0 \eta_l} \cdot (\nabla P + \rho_l g \nabla z)\right] \tag{15}$$

where

$$\xi = \frac{\rho_l}{\rho_0} \delta_{ij} e_{ij} + \frac{1}{M} P + \frac{1}{M_T} T \tag{16}$$

and

$$M = 1/\phi \beta_P \qquad M_T = 1/\phi \beta_T$$

Equation (15) is the final form of the combined mass and momentum balance law for the moving fluid in thermohydroelasticity. In isothermal conditions, (16) takes the familiar form of Biot's equation, under the assumption of solid grain incompressibility. The same assumption is used in this study in the derivation of (7). Considering the contribution of the second-order term $(e/\rho_0)(\partial \rho_l / \partial t)$ as negligible, the variable ξ can be equally termed as the equivalent fluid volume strain in nonisothermal cases. It may, therefore, be generalized for consideration of solid grain compressibility by introduction of Biot's coupling coefficient α in the following manner:

$$\xi = \frac{\rho_l}{\rho_0} \alpha \delta_{ij} e_{ij} + \frac{1}{M} P + \frac{1}{M_T} T \tag{17}$$

Equation (17) provides the first constitutive relationship for the analysis of thermohydroelastic phenomena.

The next important constitutive equation that is complementary to (17) relates the total bulk stress components τ_{ij} to strain components e_{ij}, fluid pressure P, and the thermal stress τ_{Tij}. *Biot* [1941, 1956] provides such a relationship in the absence of thermal stresses. It is known that any rise or fall of temperature acts in the form of initial strains [*Zienkiewicz*, 1976] that are independent of other mechanical stresses. Therefore, *Biot*'s [1941] stress-strain law for the mechanically isotropic case needs to be modified in the following way:

$$\tau_{ij} = 2\mu(e_{ij} - e_{Tij}) + \lambda \delta_{ij} \delta_{kl}(e_{kl} - e_{Tkl}) + \alpha \delta_{ij} P \tag{18}$$

Assuming a thermal expansivity tensor γ_{ij}, the above equation can be written as

$$\tau_{ij} = 2\mu e_{ij} + \lambda \delta_{ij} \delta_{kl} e_{kl} - \tau_{Tij} + \alpha \delta_{ij} P \tag{19}$$

where $e_{ij} = 1/2(U_{i,j} + U_{j,i})$, λ and μ are Lame's constants, and

$$\tau_{Tij} = (2\mu \gamma_{ij} + \lambda \delta_{ij} \delta_{kl} \gamma_{kl}) T \tag{20}$$

For thermal isotropy conditions, (19) can be written as

$$\tau_{ij} = 2\mu e_{ij} + \lambda \delta_{ij} \delta_{kl} e_{kl} - \beta \delta_{ij} T + \alpha \delta_{ij} P \tag{21}$$

where $\beta = (2\mu + 3\lambda)\gamma$ and γ is the isotropic linear solid thermal expansion coefficient.

The dependent variables of the above equations (i.e., e, P, and T) are all regarded as being incremental in value and represent deviation from the zero (stress-free) state. Also in the above development, thermal contact equilibrium between fluid and solid is assumed. Equations (17) and (21) provide the constitutive equations relating stresses to strain in thermohydroelasticity phenomena.

Governing equations of the phenomena are (1) the static equilibrium law given as

$$\frac{\partial \tau_{ij}}{\partial x_j} + \rho_s f_i = 0 \tag{22}$$

where f_i is the component of the body force, which is gravity in this case, (2) the law of fluid flow in porous media, given in the form of (15), and (3) the well-known law of conservation of energy, expressed in the form [*Mercer*, 1973]

$$(\rho c)_M \frac{\partial T}{\partial t} + \rho_l C_{vl} \frac{\mathbf{k}_f}{\eta_l} \cdot (\nabla P + \rho_l g \nabla z) \cdot \nabla T = \nabla \cdot \mathbf{K}_M \cdot \nabla T \tag{23}$$

where $(\rho c)_M$ and $\mathbf{K}_M$ are the specific heat capacity and thermal conductivity of the fluid-filled media, defined as

$$(\rho C)_M = \phi \rho_l C_{vl} + (1 - \phi) \rho_s C_{vs}$$

$$\mathbf{K}_M = \phi \mathbf{K}_l + (1 - \phi) \mathbf{K}_s$$

in which C_{vl} and C_{vs} are the fluid and solid specific heat constants at constant volume and $\mathbf{K}_l$ and $\mathbf{K}_s$ are the total fluid thermal dispersion tensor and the solid thermal diffusion tensor. In the development of (23) the reverse effect of temperature distribution caused by the elastic deformation of solid and dilatation of the fluid is neglected. Inclusion of the solid deformation energy, the most important of the two effects, brings about the thermoelastic coupling effect. Addition of this thermoelastic dissipation rate term, given by *Biot* [1956] as $[T_0 \beta (\partial / \partial t)](\delta_{ij} e_{ij})$, to (23) completes the energy equation:

$$(\rho c)_M \frac{\partial T}{\partial t} + T_\square \beta \frac{\partial}{\partial t}(\delta_{ij} e_{ij}) + \rho_l C_{vl} \frac{\mathbf{k}_f}{\eta_l} \cdot (\nabla P + \rho_l g \nabla z) \cdot \nabla T = \nabla \cdot \boldsymbol{K}_M \cdot \nabla T \tag{24}$$

where $T_\square$ designates the absolute temperature in the stress-free state.

Besides neglecting the energy associated with fluid dilatation, thermal contact equilibrium between fluid and solid and absence of fluid shearing stresses in the macroscopic sense are assumed. An energy source term in (24) and a mass source term in (15) are neglected for the sake of brevity. Both source terms can be added to the fluid flow and heat equation with no difficulty if so desired.

As may be seen, the fundamental laws governing the static equilibrium, flow of fluid, and flow of heat are coupled through the dependent variables of solid displacement vector, fluid pressure, and the macroscopic medium temperature. These governing laws, expressed in (15), (22), and (24), in conjunction with constitutive equations (17), (21) and the equation of state, (13), provide the complete mathematical formulation of the linear thermohydroelastic phenomena in saturated porous media. The foregoing equations, along with the following general initial and boundary conditions, define the mixed initial boundary value problem of thermohydroelasticity for which a numerical solution approach is suggested.

Initial and Boundary Conditions

The general boundary and initial conditions for the saturated porous elastic medium are

$$\begin{aligned}
\mathbf{U}(\mathbf{x}, t) &= \hat{\mathbf{U}}(\mathbf{x}, t) && \text{on} \quad A_1 \times [0, \infty) \\
\boldsymbol{\tau}(\mathbf{x}, t) \cdot \mathbf{n}(\mathbf{x}) &= \hat{\mathbf{G}}(\mathbf{x}, t) && \text{on} \quad A_2 \times [0, \infty) \\
P(\mathbf{x}, t) &= \hat{P}(\mathbf{x}, t) && \text{on} \quad B_1 \times [0, \infty) \\
\frac{\mathbf{k}_f}{\eta_l} \cdot \nabla(P + \rho_l g z) \cdot \mathbf{n}(\mathbf{x}) &= \hat{Q}_l(\mathbf{x}, t) && \text{on} \quad B_2 \times [0, \infty) \\
T(\mathbf{x}, t) &= \hat{T}(\mathbf{x}, t) && \text{on} \quad C_1 \times [0, \infty) \\
\mathbf{K}_M \cdot \nabla T \cdot \mathbf{n}(\mathbf{x}) &= \hat{Q}_h(\mathbf{x}, t) && \text{on} \quad C_2 \times [0, \infty) \\
\mathbf{U}(\mathbf{x}, 0) &= 0 && \text{on} \quad V \\
\boldsymbol{\tau}(\mathbf{x}, 0) &= 0 && \text{on} \quad V \\
P(\mathbf{x}, 0) &= 0 && \text{on} \quad V \\
T(x, 0) &= 0 && \text{on} \quad V
\end{aligned} \tag{25}$$

A, B, C represent parts of the boundary for stress-displacement, pressure-fluid flow, and temperature-heat flux considerations. The quantity V represents the volume under consideration. As mentioned earlier, the dependent variables $\mathbf{U}$, P, and T represent incremental deviations from strain-free state assumed by the above choice of initial conditions. Consideration of a different set of values for the initial conditions will necessitate replacement of $\mathbf{U}$, P, and T by $(\mathbf{U} - \mathbf{U}_0)$, $(P - P_0)$, and $(T - T_0)$ in the developed equations. Moreover, τ has to be replaced by $(\tau - \tau_0)$. In application, however, the displacement initial condition is seldom included, but this practice does not affect the results of the analysis.

Solution Approach

The degree of complexity of the thermohydroelasticity equations leaves little possibility for developing analytic solutions for even simple initial and boundary value problems. However, numerical solutions to the most general initial and boundary value problems can rather easily be found. Various numerical schemes, such as finite element and finite difference methods, can be utilized. In this work the finite element technique is used. A mixed variational and Galerkin finite element method forms the basis of this approach.

Variational Formulation

The variational method is used to formulate the hydroelastic part of the thermohydroelastic phenomena.

Let $R = \{\mathbf{U}, P\}$ be an admissible state in J defined in $V \times [0, \infty)$, and let the functions $\mathbf{U}$ and P possess the appropriate continuity and differentiability conditions. J is the set of all admissible states, V is the region of space occupied by the fluid-porous solid mixture. A function $\Omega_t(R)$ over J for each time $t \in [0, \infty)$ is defined as

$$\begin{aligned}
\Omega_t(R) = \int_V & (e_{ij} * C_{ijkl} e_{kl} - 2T * \beta \delta_{ij} e_{ij} - 2\rho_s f_i * U_i \\
& + 2P * \frac{\alpha \rho_l}{\rho_0} \delta_{ij} e_{ij} - 1 * \nabla P * \frac{\mathbf{k}_f}{\eta_l} \nabla P \\
& - P * \frac{1}{M} P - P * \frac{1}{M_T} T \\
& + 2 * \rho_l g \nabla z * \frac{\mathbf{k}_f}{\eta_l} \nabla P)\, dv - 2 \int_{A_2} \hat{G}_i * U_i \, ds \\
& - 2 \int_{B_2} 1 * \hat{Q}_l * P ds
\end{aligned} \tag{26}$$

where the asterisk denotes convolution product and C_{ijkl} represents the elasticity tensor. It can be shown that

$$\delta_{\bar{R}} \Omega(R) = \frac{d}{dv} \Omega(R + v\bar{R}) \bigg|_{v=0} = 0 \qquad \text{for every } \bar{R} \in J$$

if and only if R is a solution state of the mixed boundary value problem. The presence of temperature terms in the variational principle is also justified physically by the fact that thermal effects act in the form of initial strains, as explained earlier.

Galerkin Formulation

A Galerkin method is used to obtain a numerical formulation for the energy equation. Choosing approximating functions of the form $T = \boldsymbol{\Phi} \boldsymbol{T}$, where Φ_i represents the ith basis functions and T_i denotes the discrete temperature values to be determined, the Galerkin procedure, modified by the application of Green's second theorem, requires the following:

$$\int_V \left\{ (\rho C)_M \Phi_i \frac{\partial T}{\partial t} + \beta T_0 \Phi_i \frac{\partial}{\partial t}(\delta_{ij} e_{ij}) + \rho_l C_{vl} \Phi_i \mathbf{q} \cdot \nabla T + \nabla \Phi_i \cdot \mathbf{K}_M \cdot \nabla T \right\} dv - \int_{C_2} \Phi_i \hat{Q}_h \, ds = 0 \tag{27}$$

where the volume integral in (27) represents a global restatement of (24) and the surface integral indicates the global satisfaction of the heat flux boundary condition [*Hsu and Nickell*, 1974].

Finite Element Discretization

The field variables, the displacement vector $\mathbf{U}$, the pressure P, and the temperature T, are interpolated as follows:

$$\begin{aligned}
\mathbf{U} &= \boldsymbol{\Phi}_u^{T_r} \mathbf{U} \\
P &= \boldsymbol{\Phi}^{T_r} P \\
T &= \boldsymbol{\Phi}^{T_r} T
\end{aligned} \tag{28}$$

where T_r stands for matrix transpose operation and the Φ_i are piecewise continuous polynomial functions that are used in conjunction with the mixed isoparametric quadrilateral elements. Proper substitution of (28) and related derivatives of Φ_u and Φ represented by Φ_e and Φ_θ in the Galerkin integral and the functional, after taking variations with respect to U and P for the functional, yields the following matrix finite element formulation:

$$\mathbf{KU} + \mathbf{C}_{UP}\mathbf{P} + \mathbf{C}_{UT}\mathbf{T} = \mathbf{F} \tag{29}$$

$$\mathbf{C}_{PU}\mathbf{U} + (\mathbf{E}_f + 1*\mathbf{H}_f)\mathbf{P} + \mathbf{C}_{PT}\mathbf{T} = -1*\mathbf{Q}_l \tag{30}$$

$$\mathbf{C}_{TU}\mathbf{U} + [\mathbf{E}_h + 1*(\mathbf{H}_{hf} + \mathbf{H}_h)]\mathbf{T} = -1*\mathbf{Q}_h \tag{31}$$

where 1* represents time integration. Matrix coefficients of above formulation are presented in the appendix.

Solution Scheme

Two different schemes of time integration are used to integrate the matrix equations (29), (30), and (31). A predictor-corrector scheme [*Taylor*, 1974] is used for the integration of the first two implicitly coupled equations [*Ayatollahi*, 1978]. For the energy equation the Crank-Nicolson step-by-step procedure is used, where the solution of each step is sought in the middle of the interval. The solution technique for both symmetric and nonsymmetric matrices, finalized in the above procedures, is the *LU* decomposition Gaussian method.

The coupling of (31) and (30) is nonlinear and is implicitly expressed in $\mathbf{H}_{hf}$, the nonsymmetric convective thermal conductivity matrix. The large time constant of the energy equation, as compared to that of the flow equation, makes the above presentation of the numerical equations quite attractive for an interlacing scheme of solutions such as used by *Sorey* [1975]. This interlacing scheme uses the fluid velocity obtained from a direct solution of (29) and (30) and feeds back the temperature resulting from solution of (31) to the first equation pair to repeat the cycle. Quasi-linearization of temperature dependent material properties is embedded in this procedure. This approach of solving the coupled equations is enhanced by the low sensitivity of the dependent variables P and U within some ranges of temperature in different problems. Therefore energy equations in these ranges can march through time using large time steps compared to the small time steps required in the simultaneous solving of the other two equations. This scheme has still further advantages in situations where the mass transfer contribution to temperature distribution is negligible. In these cases a single solution of the energy equation provides the needed temperature information for the stepwise solution of the other two equations.

However, the present formulation of the coupled equations (29), (30), and (31) needs to be altered if a one-step direct solution (fully implicite) is desired, as opposed to the interlaced solution. To obtain a useful form, a Crank-Nicolson approximation to (31) is used and the following manipulation is performed:

$$\nabla P \cdot \nabla T = \tfrac{1}{2}P_t{}^{Tr}\Phi_\theta\Phi_\theta{}^{Tr}\mathbf{T}_{t+\Delta t} + \tfrac{1}{2}T_t{}^{Tr}\Phi_\theta\Phi_\theta{}^{Tr}\mathbf{P}_{t+\Delta t}$$

where $\nabla P = \Phi_\theta{}^{Tr}\mathbf{P}$, $\nabla T = \Phi_\theta{}^{Tr}\mathbf{T}$, and $\Delta P \Delta T$ is neglected. As a result, the new matrix representation of energy equation will be of the form

$$\mathbf{C}_{TU}U + (1*\mathbf{C}_{TP})\mathbf{P} + (\mathbf{E}_h + 1*\mathbf{H}_h')\mathbf{T} = -1*\mathbf{Q}_h \tag{32}$$

where $\mathbf{C}_{TP}$ and $\mathbf{H}_h'$ are defined as

$$\mathbf{C}_{TP} = \sum_{n=1}^{N}\frac{1}{2}\int_{v^n}\mathbf{T}_t{}^{nTr}\Phi_\theta{}^n\Phi_\theta{}^{nTr}\,dv^n$$

$$\mathbf{H}_h' = \mathbf{H}_h + \sum_{n=1}^{N}\frac{1}{2}\int_{v^n}\mathbf{P}_t{}^{nTr}\Phi_\theta{}^n\Phi_\theta{}^{nTr}\,dv^n$$

Now accurate direct solution of (29), (30), and (32) can be properly handled. It is important to notice that the total system matrix is nonsymmetric and of much larger order; therefore, in the one-step solution approach some computer solution efficiency is lost in comparison with the interlacing solution scheme. However, at the expense of increased solution time, the required computer storage might be reduced by the use of schemes [*Hsu and Nickell*, 1974] that make the system matrix symmetric.

In the above development the medium was assumed to behave linearly with respect to all physical properties under consideration. However, at this point the stage is set for the introduction of material nonlinearities to the numerical approach presented here. At present, the nonlinearities considered in this work are limited to those brought about by the introduction of fractures in the problem domain and those originating from the thermal dependency of physical properties. Following the common practice [*Zienkiewicz*, 1976], no major basic change of the numerical method is needed. Fractures are represented by two nodal point line elements [*Wilson and Witherspoon*, 1970] for flow modeling and by four nodal point joint (line) elements [*Goodman et al.*, 1968] for mechanical modeling. The hydromechanical nonlinearity, caused by fracture deformability, is treated by a secant iteration scheme within each time step. Details regarding the introduction of fracture elements are thoroughly covered in an earlier paper [*Noorishad et al.*, 1982*a*]. As far as thermal nonlinear effects are concerned, the quasi-linearization approach used in our interlaced method allows for a proper treatment in most situations. In cases of severe nonlinearities, iterations in each cycle can be performed.

VERIFICATION AND APPLICATION

Because other methods were not available, full-capability verification of ROCMAS was not possible for some time. Earlier publications [*Witherspoon et al.*, 1981*b*] provide an account of partial testings of the code. A recent publication by *Aboustit et al.* [1982], however, provided an opportunity for the code-to-code verification that is presented below. An attempt is made here in a scoping study to simulate the effect of the emplacement of a thermal source in a fluid-saturated, fractured rock environment.

TABLE 1. Data Used in Sand Column Consolidation Analysis

Property	Value
Porosity, ϕ	2.0×10^{-1}
Young's modulus,* E_s	6×10^3 Pa
Poisson's ratio, ν_s	4.0×10^{-1}
Thermal expansion coefficient, β_T	3.0×10^{-7}
Matrix heat capacity, ρC	167.2 kJ/m^3 °C
Solid-fluid-thermal conductivity, K_M	8.36×10^{-1} kJ/m s °C
Permeability,† k_f	4.0×10^{-6} m/s
Biot's coupling coefficient, α	1.0

Material is rock.
*See notation section for relationship with Lame's constants.
†Fluid properties are assumed to be constant in this problem.

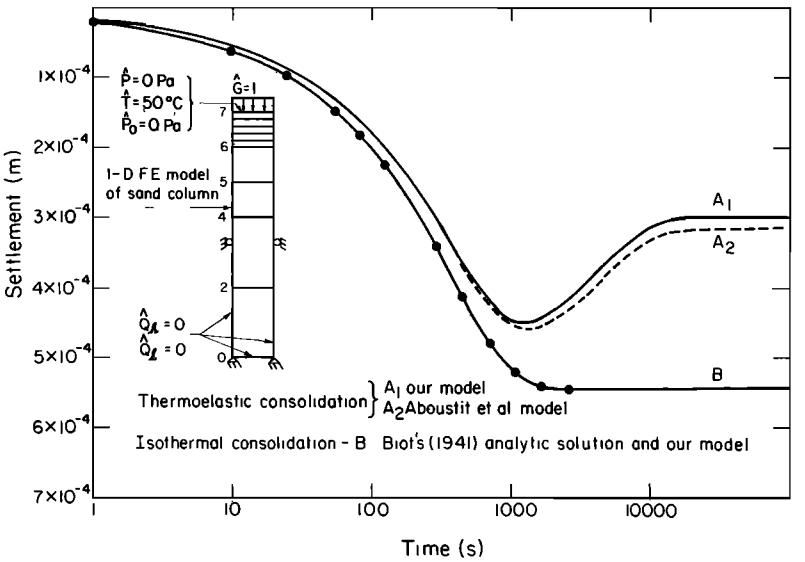

Fig. 1. Consolidation history for the one-dimensional finite element model.

Verification: Thermoelastic Consolidation of a Sand Column

Aboustit et al. [1982] used a nonconvective coupled variational finite element approach to analyze the thermoelastic consolidation of a sand column. Table 1 gives the data used in this problem. Results of their analysis have been reproduced in Figure 1 along with our solution of the same problem. There is almost perfect agreement between the two solutions. The slight discrepancy is due to the interlaced solution scheme of the present work, in which temperature solution lags one step behind the hydromechanical calculations. Reduction of the time step size will decrease the difference. In solving this problem, the advection of energy along with the effects of fluid compressibility, thermal expansivity, and viscosity variations were assumed to be negligible. All of these assumptions, in addition to linear material behavior, can be relaxed at will in the program ROCMAS.

TABLE 2. Data Used for Analysis of Fracture Inflow to a Heater Borehole

Material	Property	Value
Rock	mass density, ρ_s	2.6×10^3 kg/m^3
	porosity, ϕ	5.0×10^{-2}
	Young's modulus, E_s	51.3 GPa
	Poisson's ratio, ν_s	0.23
	thermal expansion coefficient, β_t	8.8×10^{-5} C°$^{-1}$
	specific heat, C_{vs}	2.1×10^{-1} kJ/kg °C
	thermal conductivity, K_M	3.18×10^{-3} kJ/m s °C
	permeability, k_f	1.0×10^{-18} m^2
	Biot's storativity constant, $1/M$	5.0 GPa
	Biot's coupling constant, α	1.0
Fracture	initial aperture, $2b$	10^{-1} m
	Biot's storativity constant, $1/M$	5.0 GPa
	initial normal stiffness, K_N	85 GPa/m
	initial tangential stiffness, K_S	0.85 MPa/m
	friction angle, ψ	30°
	cohesion, C	0.0
	porosity, ϕ	1.0

The developments presented in this paper do not contain the expansions needed for the inclusion of the nonlinear fracture element, for the sake of brievity. However, as it was explained in the text, this task has been performed along the lines of *Noorishad et al.* [1982*a*], and the ROCMAS code can handle porous fractured rocks.

Application: A Scoping Analysis of the Occurrence of Coupled Thermal-Hydraulic-Mechanical Phenomena Near a Heater

To demonstrate the ability of ROCMAS to simulate the thermohydromechanical environment around a waste canister or heater, the changes of fluid inflow to a heater borehole induced by the temperature rise are studied. A 5-kW heater is located at a depth of 350 m in granite. A horizontal fracture is assumed to lie 3 m below the heater midplane and extend from the heater borehole to a hydrostatic boundary at a radial distance of 20 m from the borehole. The properties of rock

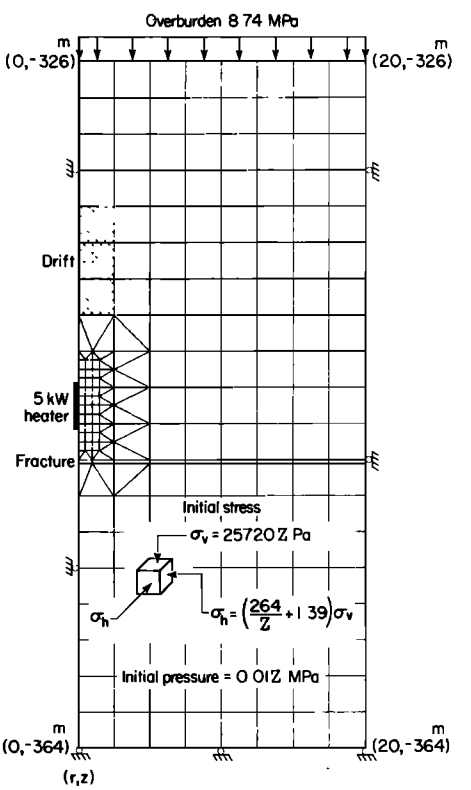

Fig. 2. Finite element model of the heat source environment.

and fracture are given in Table 2, and the two-dimensional axisymmetric (r, z) finite element grid is shown in Figure 2. The heater drift, approximated by the cylindrical hatched area, is simulated by assigning a very low value of Young's modulus to the elements. Before the heater raises the temperature of a large volume of the rock, the flow from the hydrostatic outer boundary to the atmospheric ("zero" hydraulic pressure) borehole is high. Later in time, with the heated rock above the fracture expanding and the fracture aperture near the heater borehole closing, the flow decreases sharply, as shown in Figure 3. The evolution of the fracture aperture profile, together with the variations of the pressure and temperature distributions, are shown in Figure 4. As may be seen, in the pressure-distance graph of this figure, at 0 day, before the tapping of the fracture, full hydrostatic pressure prevails in the fracture. This pressure diminishes rapidly at 0.25 day before major development of the thermal front. However, as thermal stresses are established, the fracture starts closing. As a result, the pressure inside the fracture starts rising, thus leading to the establishment of full pressure in the fracture at 14 day, similar to the 0 day case. These results may provide a better understanding of some of the observations made in the in situ heater experiments in the Stripa granite. The delayed responses of the extensometers in these experiments [*Witherspoon et al.*, 1981*a*] may be explained by the closing of the fracture. Similarly, reduction leading to stoppage of the water inflows into the heater boreholes [*Nelson et al.*, 1981] can also be explained by the same phenomena.

CONCLUSIONS

The work presented here provides a new technique for investigation of thermal-hydraulic-mechanical behavior of fractured porous rocks. The work is based on the fundamentals of consolidation and thermoelasticity, which are recast into what we call thermohydroelasticity theory.

A direct solution process has been employed that involves a variational formulation and a Galerkin integral to produce a set of three matrix equations. In this presentation the equations of static equilibrium and fluid flow appear in an implicitly coupled form, and the energy equation is explicitly coupled to these equations. In this scheme, referred to as the interlacing scheme, a compatible solution is obtained. To prepare the formulation for a complete direct solution scheme, the Crank-Nicolson approximation is introduced in the energy equation, and as a result, the energy equation also becomes linearly coupled to the other two equations. An account of the partial verification of the developed code ROCMAS can be found in the work by *Witherspoon et al.* [1981*b*]. In this paper, the results of a code-to-code verification of the triple analysis capability of ROCMAS are presented for the first time. Also, in a scoping analysis, thermohydromechanical simulation of fracture inflow near a heater was performed. It was illustrated that the nonlinear fracture behavior activated by coupling effects can change fluid flow behavior in the rock dramatically.

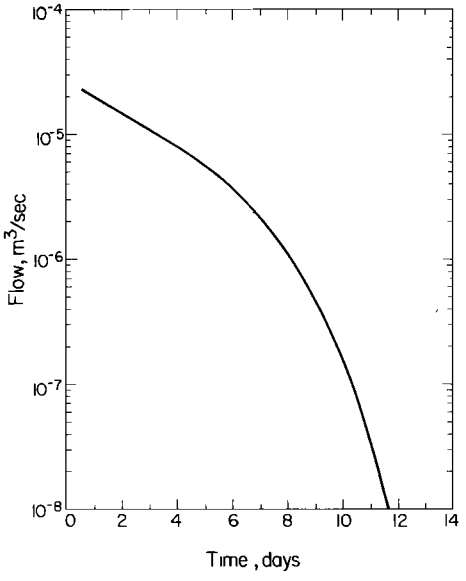

Fig. 3. Variation of fluid inflow to the heater borehole as a function of time.

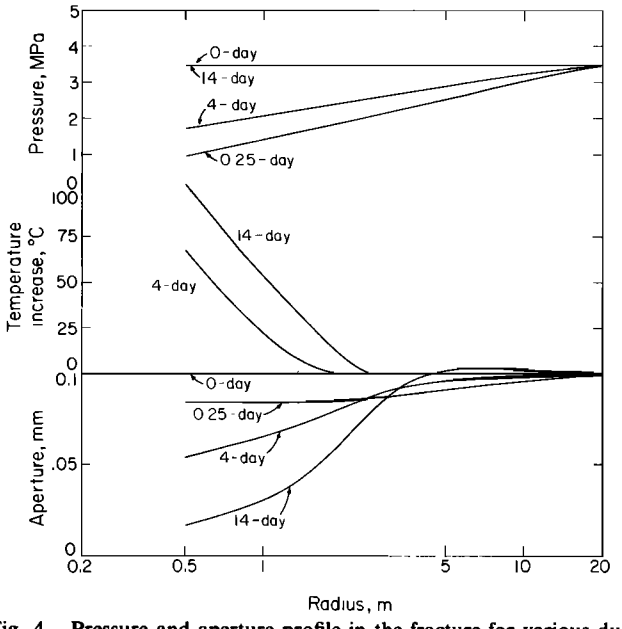

Fig. 4. Pressure and aperture profile in the fracture for various durations and temperature profiles along the heater midplane.

APPENDIX: MATRIX COEFFICIENTS OF EQUATIONS (29), (30), AND (31)

Matrix coefficients of the solution formulation (equations (29), (30), and (31)) are defined in the following equations:

$$\mathbf{K} = \sum_{n=1}^{N} \int_{v^n} \Phi_e{}^n \mathbf{C}^n \Phi_e{}^{nTr}\, dv^n$$

$$\mathbf{C}_{PU} = \mathbf{C}_{UP}{}^{Tr} = \sum_{n=1}^{N} \int_{v^n} \Phi^n \frac{\alpha^n \rho_l{}^n}{\rho_0{}^n} \hat{\mathbf{1}} \Phi_e{}^{nTr}\, dv^n$$

$$\mathbf{C}_{UT} = \sum_{n=1}^{N} \int_{v^n} \Phi^n \beta \hat{\mathbf{1}} \Phi_e{}^{nTr}\, dv^n$$

$$\mathbf{C}_{TU} = \frac{1}{T_\square}\, \mathbf{C}_{UT}{}^{Tr}$$

$$\mathbf{E}_f = \sum_{n=1}^{N} \int_{v^n} \Phi^n \frac{1}{M^n} \Phi^{nTr}\, dv^n$$

$$\mathbf{H}_f = \sum_{n=1}^{N} \int_{v^n} \Phi_\theta{}^n \frac{\mathbf{k}_f{}^n}{\eta_l} \Phi_\theta{}^{nTr}\, dv^n$$

$$\mathbf{C}_{PT} = \sum_{n=1}^{N} \int_{v^n} \Phi^n \frac{1}{M_T{}^n} \Phi^{nTr}\, dv^n$$

$$\mathbf{E}_h = \sum_{n=1}^{N} \int_{v^n} \mathbf{\Phi}^n (\rho C)_M{}^n \mathbf{\Phi}^{nTr}\, dv^n$$

$$\mathbf{H}_{hf} = \sum_{n=1}^{N} \int_{v^n} \mathbf{\Phi}^n (\phi \rho_{0l} C_{vl})^n \mathbf{q} \mathbf{\Phi}_\theta{}^{nTr}\, dv^n$$

$$\mathbf{H}_h = \sum_{n=1}^{N} \int_{v^n} \mathbf{\Phi}_\theta{}^n \mathbf{K}_M{}^n \mathbf{\Phi}_\theta{}^{nTr}\, dv^n$$

$$\mathbf{Q}_f = \sum_{n=1}^{n_1} \int_{B_2{}^n} \mathbf{\Phi}^n \mathbf{\Phi}^{nTr} \hat{Q}_f{}^n\, ds^n + \sum_{n=1}^{N} \int_{v^n} \mathbf{\Phi}_\theta \frac{\mathbf{k}_f}{\eta_l} \rho_l g \hat{\mathbf{1}}_z\, dv^n$$

$$\mathbf{Q}_h = \sum_{n=1}^{n_2} \int_{C_2{}^n} \mathbf{\Phi}^n \mathbf{\Phi}^{nTr} \hat{Q}_h{}^n\, ds^n$$

$$\mathbf{F} = \sum_{n=1}^{n_3} \int_{A_2{}^n} \mathbf{\Phi}_u{}^n \mathbf{\Phi}_u{}^{nTr} \hat{\mathbf{G}}\, ds^n + \sum_{n=1}^{N} \int_{v^n} \mathbf{\Phi}_u{}^n \rho_s{}^n g \hat{\mathbf{1}}_z\, dv^n$$

where

$$\hat{\mathbf{1}} = \begin{Bmatrix} 1 \\ 1 \\ 1 \\ 0 \\ 0 \\ 0 \end{Bmatrix} \qquad \hat{\mathbf{1}}_z = \begin{Bmatrix} 0 \\ 0 \\ 1 \end{Bmatrix}$$

The superscript Tr stands for matrix transposition operation; n_1, n_2, and n_3 designate parts of A_2, B_2, and C_2 boundary surfaces, respectively.

NOTATION

A_1, A_2 structural boundaries where displacements and surface tractions are prescribed.
B_1, B_2, C_1, C_2 fluid flow and heat flow boundary parts where Dirichlet or Neuman boundary conditions are prescribed.
$\mathbf{C}$ elasticity matrix.
C_{ijkl} components of elasticity tensor for solid phase.
$\mathbf{C}_{PT}$ pressure-temperature coupling matrix.
$\mathbf{C}_{UP}$ displacement-pressure coupling matrix.
$\mathbf{C}_{UT}$ displacement-temperature coupling matrix.
C_{vl} specific heat capacity of liquid at constant volume.
C_{vs} specific heat capacity of solid at constant volume.
$D/D^s t$ comoving time derivative following solid motion.
e_{ij} components of strain tensor for solid phase.
E Young's modulus, $\mu(3\lambda + 2\mu)/(\lambda + \mu)$.
$\mathbf{E}_f$ fluid storativity matrix.
$\mathbf{E}_h$ heat capacity matrix.
f_i components of body force vector.
$\mathbf{F}$ force vector.
g gravitational acceleration.
$\hat{\mathbf{G}}$ traction vector on A_2 boundary.
$\mathbf{H}_f$ fluid conductivity matrix.
$\mathbf{H}_h$ heat conductivity matrix.
$\mathbf{H}_{hf}$ mass transfer conductivity matrix.
$\mathbf{k}_f$ intrinsic permeability tensor.
K stiffness matrix.
$\mathbf{K}_l$ liquid thermal conductivity tensor.
$\mathbf{K}_M$ solid-fluid mixture thermal conductivity tensor.
$\mathbf{K}_s$ solid thermal conductivity tensor.
M Biot's constant, $1/\phi\beta_P$.
M_T constant, $1/\phi\beta_T$.
N total number of elements in finite element idealization.
$\mathbf{n}$ outward normal direction cosine vector.
n index used to designate element number.
P pressure.
$\mathbf{P}$ pressure vector.
$\mathbf{P}_t$ element pressure vector at preceding time step.
$\mathbf{q}$ fluid flow vector.
$\mathbf{Q}_h$ heat flow vector.
$\mathbf{Q}_l$ fluid flow vector.
$\hat{Q}_l$ normal fluid outflow from B_2 boundary.
T temperature.
$T_\square$ absolute temperature in stress-strain free state.
Tr matrix transpose sign.
$\mathbf{T}$ temperature vector.
$\mathbf{T}_t$ element temperature vector at preceding time step.
$\mathbf{U}$, $\mathbf{U}_s$ solid element displacement vector.
$\mathbf{U}_l$, $\mathbf{V}_l$ liquid displacement and velocity vectors.
$\mathbf{V}_s$ solid velocity vector.
V space occupied by fluid-solid mixture.
v^n region of space occupied by fluid-solid mixture of an element n.
x_i or x, y, z Cartesian coordinates, $i = 1, 2, 3$.
α Biot hydroelastic coupling coefficient.
β thermoelastic coupling coefficient, equal to $(2\mu + 3\lambda)\gamma$.
β_P fluid compressibility.
β_T fluid thermal expansion coefficient.
γ solid thermal expansion coefficient.
δ_{ij} Kronecker delta function.
Δ first order difference operator.
η_l liquid dynamic viscosity.
λ Lamé's elasticity constant.
μ Lamé's elasticity constant.
ν functional perturbation parameter.
ν_s Poisson's ratio, $\lambda/2(\lambda + \mu)$.
ξ fluid volume strain.
ρ_l, $\hat{\rho}_l$ liquid mass density and average liquid mass density.
ρ_s, $\hat{\rho}_s$ solid mass density and average solid mass density of porous space.
ρ_M solid-fluid mixture mass density.
$(\rho C)_M$ solid-fluid mixture heat capacity.
τ, τ_{ij} stress tensor and components (compression negative).
τ_T, τ_{Tij} thermal stress tensor and components.
ϕ porosity.
$\mathbf{\Phi}_u$ displacement interpolation function matrix.
$\mathbf{\Phi}_e$ strain-nodal displacement transformation matrix.
$\mathbf{\Phi}$ pressure and temperature interpolation function matrix.
$\mathbf{\Phi}_\theta$ transformation matrix for pressure or temperature gradients.
ψ fracture friction angle.
$\hat{}$ signifies assigned boundary conditions or average values of some thermodynamic quantity.
0 signifies initial conditions
$*$ time convolution sign

Acknowledgments. This paper was prepared under the auspices of the Director, Office of Energy Research, Office of Basic Energy Sciences, Division of Engineering, and Geosciences of the U.S. Department of Energy under contract DE-AC03-76SE00098 and the Waste Management Branch, Division of Radiation Programs and Earth Sciences, Office of Nuclear Regulatory Research, U.S. Nuclear Regulatory Commission, Washington D. C., 20555 through NRC Fin B 3046-3 under Interagency Agreements DOE-60-83-388 and 60-83-367.

REFERENCES

Aboustit, B. L., S. H. Advani, J. K. Lee, and R. S. Sandhu, Finite element evaluation of thermo-elastic consolidation, *Proc. U.S. Symp. Rock Mech., 23rd*, 587–595, 1982.

Aifantis, E. C., Introducing a multi-porous medium, *Dev. Mech., 9*, 209–211, 1977.

Atherton, R. W., E. J. Finnemore, M. L. Gillam, A. E. Degance, G. A. Nystrom, and R. B. Schainker, The analysis of subsidence associated with geothermal development, vol. II, Research Report, prepared for National Science Foundation/RANN, grant AER75-17298, *Rep. 5139-2*, System Control Inc., Palo Alto, Calif., 1976.

Ayatollahi, M. S., Stress and flow in fractured porous media, Ph.D. thesis, Univ. of Calif., Berkeley, 1978.

Baca, R. G., Coupled geomechanical/hydrological modeling: An overview of BWIP studies, Proceedings of the ONWI Workshop on Thermomechanical-Hydrochemical Modeling for a Hard Rock Waste Repository, *Rep. LBL-11204*, Lawrence Berkeley Lab., Berkeley, Calif., 1980.

Bear, J., and M. Y. Corapcioglu, A mathematical model for consolidation in a thermoelastic aquifer due to hot water injection or pumping, *Water Resour. Res., 17*(3), 723–736, 1981.

Biot, M. A., General theory of three-dimensional consolidation, *J. Appl. Phys., 12*, 144–164, 1941.

Biot, M. A., Thermoelasticity and irreversible thermodynamics, *J. Appl. Phys., 27*, 240–253, 1956.

Crochet, M. J., and P. M. Naghdi, On constitutive equations for flow of fluid through an elastic solid, *Int. J. Eng. Sci., 4*, 383–401, 1966.

Davis, S. N., and G. W. Moore, Semidiurnal movement along a bedrock joint in Wool Hollow Cave, California, *NSS Bull., 27*(4), 133–142, 1965.

Evans, D. M., The Denver area eqrthquake and Rocky Mountain Arsenal Well, *Mt. Geol., 3*(1), 23–36, 1966.

Freeze, R. A., and Cherry, J. N., *Groundwater*, Prentice-Hall, Englewood Cliffs, N.J., 1979.

Gale, J. E., A numerical field and laboratory study of flow in rocks with deformable fractures, Ph.D. thesis, Univ. of Calif., Berkeley, 1975.

Ghaboussi, J., and E. L. Wilson, Flow of compressible fluid in porous elastic media, *Int. J. Numer. Methods Eng., 5*, 419–442, 1973.

Goodman, R. E., R. L. Taylor, and T. Brekke, A model for the mechanics of jointed rock, *J. Soil Mech. Found. Div. Am. Soc. Civ. Eng., 94*(SM3), 637–659, 1968.

Green, A. E., and P. M. Naghdi, A dynamical theory of interacting continua, *Int. J. Eng., Sci., 3*, 231–241, 1965.

Gurtin, M., Variational principles for linear initial-value problems, *Q. Appl. Math., 22*(3), 252, 1964.

Helm, D. C., Evaluation of stress-dependent aquitard parameters by simulating observed compaction from known stress history, Ph.D. thesis, Univ. of Calif., Berkeley, 1974.

Hocking, G., Thermochanical modeling for hardrock: Status and needs, Proceedings of the Workshop on Thermomechanical Modeling for a Hardrock Waste Repository, *Rep. UCAR-10043*, Lawrence Livermore Lab., Livermore, Calif., 1979.

Hsu, M. B., and Nickell, R. E., Coupled convective and conductive heat transfer by finite element method, *Finite Element Methods in Flow Problems*, edited by J. T. Oden, O. C. Zienkiewicz, R. H. Gallagher, and C. Taylor, pp. 427–450, UAH Press, Huntsville, Ala., 1974.

Louis, C., and Y. N. T. Maini, Determination of in-situ hydraulic parameters in jointed rock, in *Proceedings Second Congress International Society for Rock Mechanics*, pp. 1–32, Privredni Pregled, Belgrade, 1970.

Mercer, J. W., Finite-element approach to the modeling of hydrothermal systems, Ph.D. thesis, Univ. of Ill., Urbana-Champaign, 1973.

Miller, I., W. Dershowitz, K. Jones, L. Myer, K. Roman, and M. Schaver, Simulation of geothermal subsidence, *Rep. LBL-10794*, Lawrence Berkeley Lab., Berkeley, Calif., 1980.

Narasimhan, T. N., and P. A. Witherspoon, Numerical model for saturated-unsaturated flow in deformable porous media, 1, Theory, *Water Resour. Res., 13*(3), 657–664, 1977.

Nelson, P. H., R. Rachiele, and J. S. Remer, Water inflow into boreholes during the Stripa heater experiments, *Rep. LBL-12574*, Lawrence Berkeley Lab., Berkeley, Calif., 1981.

Noorishad, J., Finite-element analysis of rock mass behavior under coupled action of body forces, flow forces, and external loads, Ph.D. thesis, Univ. of Calif., Berkeley, 1971.

Noorishad, J., M. S. Ayatollahi, and P. A. Witherspoon, A finite element method for coupled stress and fluid flow analysis of fractured rocks, *Int. J. Rock Mech. Sci., 19*, 185–193, 1982*a*.

Noorishad, J., M. Mehran, and T. N. Narasimhan, On the formulation of saturated-unsaturated fluid flow in deformable porous media, *Adv. Water Resour., 5*, 588–596, 1982*b*.

Pinder, G. F., State-of-the-art review of geothermal reservoir modeling, *Rep. LBL-9093*, Lawrence Berkeley Lab., Berkeley, Calif., 1979.

Pritchett, J. W., S. K. Garg, D. H. Brownell, Jr., and H. B. Levine, Geohydrological environment effects of geothermal power production phase I, *Rep. SSS-R-75-2733*, Syst. Sci. and Software, La Jolla, Calif., 1975.

Safai, N. M., and G. F. Pinder, Vertical and horizontal land deformation in a desaturating porous medium, *Adv. Water Resour., 2*, 19–25, 1979.

Sandhu, R. S., and E. L. Wilson, Finite-element analysis of seepage in elastic media, *J. Eng. Mech. Div. Am. Soc. Civ. Eng., 95*(EM3), 641–652, 1969.

Snow, D. T., A parallel plate model of fractured permeable media, Ph.D. thesis, Univ. of Calif., Berkeley, 1965.

Snow, D. T., Fracture deformation and changes of permeability and storage upon changes of fluid pressure, *Q. Colo. Sch. Mines, 63*(1), 201, 1968.

Sorey, M. L., Numerical modeling of liquid geothermal systems, Ph.D. thesis, Univ. of Calif., Berkeley, 1975.

Taylor, R. L., Analysis of flow of compressible or incompressible fluids in porous elastic solids, consulting report to the Naval Civil Engineering Laboratory, Port Hueneme, Calif., 1974.

Terzaghi, K., *Erdbaumechanik auf bodenphsikalischer Grundlage*, F. Deuticke, Leipzig, 1925.

Theis, C.. V., The significance and nature of the cone of depression in groundwater bodies, *Econ. Geol., 33*, 889–902, 1938.

Tsang, C. F., A review of the state of the art of thermomechanical-hydrochemical modeling of a hardrock waste repository. Proceeding ONWI Workshop on Thermomechanical-Hydrochemical Modeling for a Hardrock Waste Repository, *Rep. LBL-11204*, Lawrence Berkeley Lab., Berkeley, Calif., 1980.

Van Poollen, H. K., Report of pumping tests, Rocky Mountain Arsonal disposal well, September–October 1968, U.S. Army Corps of Eng., Omaha, Nebr., 1969.

Wang, J. S. Y., R. Sterbentz, and C. F. Tsang, The state of the art of numerical modeling of thermohydrologic flow in fractured rock masses, *Rep. LBL-10524*, Lawrence Berkeley Lab., Berkeley, Calif., 1980.

Weeks, E. P., Aquifer tests—The state of the art in hydrology, Proceedings, Invitational Well-Testing Symposium, *Rep. LBL-7027*, pp. 14–26, Lawrence Berkeley Lab., Berkeley, Calif., pp. 14–26, 1977.

Wilson, C. R., and P. A. Witherspoon, An investigation of laminar flow in fractured rocks, *Geotech. Rep. 70-6*, Univ. of Calif., Berkeley, 1970.

Witherspoon, P. A., N. G. W. Cook, and J. E. Gale, Geologic storage of radioactive waste, field studies in Sweden, *Science, 211*, 894–900, 1981*a*.

Witherspoon, P. A., J. Long, Y. Tsang, J. Noorishad, New approaches to the problem of fluid flow in fractured rock masses, *Proc. U.S. Congr. Rock Mech., 22nd*, 1–20, 1981*b*.

Zienkiewicz, O. C., *The Finite-Element Method in Structural and Continuum Mechanics*, McGraw-Hill, New York, 1976.

J. Noorishad, C. F. Tsang, and P. A. Witherspoon, Earth Sciences Division, Lawrence Berkeley Laboratory, 1 Cyclotron Road, Berkeley, CA 94720.

(Received August 15, 1983;
revised July 10, 1984;
accepted July 17, 1984.)